Carrier Capture and Escape Times in $In_{0.35}Ga_{0.65}As$–GaAs Multiquantum-Well Lasers Determined from High-Frequency Electrical Impedance Measurements

I. Esquivias, *Member, IEEE,* S. Weisser, B. Romero, J. D. Ralston, *Member, IEEE,* and J. Rosenzweig

***Abstract*— We present experimental results on the high-frequency electrical impedance of $In_{0.35}Ga_{0.65}As$–GaAs multiquantum-well lasers with varied p-doping levels in the active region. The analysis of the data, using a simple three rate equation model, provides information about the dynamical time constants (the carrier lifetime, the effective carrier capture and escape times) under the laser operation conditions. The addition of p-doping increases the carrier escape time at threshold from 0.7 ns, extracted for the undoped devices, up to a value higher than 2 ns for the p-doped lasers. The effective capture time is estimated to be between 2 and 5 ps.**

THE TRANSPORT of carriers across the confinement region, the carrier capture into, and the carrier escape out of the quantum wells (QW's) are very important processes for understanding the dc and high-frequency properties of QW lasers [1]–[5].The most usual rate equation models considering these processes [1]–[4] describe the carrier transport/capture and escape rates using effective transport/capture and escape times, $\tau_{\rm cap}$ and $\tau_{\rm esc}$, respectively. A good knowledge of $\tau_{\rm cap}$ and $\tau_{\rm esc}$ at the injection levels used in present laser structures is necessary to consider the influence of these processes on the laser performance.

We have recently demonstrated [4], [5] that high-frequency electrical impedance (HFEI) and modulation response (MR) measurements can provide valuable information about the carrier dynamics at the laser operating conditions. Our results indicated that a simple "three-rate-equation" model, considering the effective parameters $\tau_{\rm cap}$ and $\tau_{\rm esc}$, and including the space-charge capacitance $C_{\rm sc}$, is accurate enough for describing the experimental behavior of ultra-high-speed lasers (up to 30 GHz modulation bandwidth). Moreover, HFEI measurements in the subthreshold regime are a powerful tool for determining $\tau_{\rm esc}$ and $\tau_{\rm eff}$, the effective lifetime of carriers in the QW's, when the values of these time constants are comparable. In this letter we present and evaluate HFEI measurements for $In_{0.35}Ga_{0.65}As$–GaAs MQW lasers with varied p-doping concentrations in the active region. The current dependence of the dynamic time constants ($\tau_{\rm esc}$, $\tau_{\rm eff}$, and τ_o, a time constant associated to $\tau_{\rm cap}$ and $C_{\rm sc}$ [4]) is determined and discussed.

Manuscript received May 23, 1996. This work was supported by the Bundesministerium für Bildung, Wissenschaft, Forshung und Technologie. The work of I. Esquivias and B. Romero was supported by Comisión Interministerial de Ciencia y Tecnología (Spain), Project TIC95-0563-C05.

I. Esquivias and B. Romero are with the Departamento de Tecnología Fotónica, Universidad Politécnica de Madrid, Ciudad Universitaria, E-28040, Madrid, Spain.

S. Weisser, and J. Rosenzweig are with the Fraunhofer Institut Angewandte Festkörperphysik, Tullastrasse 72, D-79108 Freiburg, Germany.

J. D. Ralston was with the Fraunhofer Institut Angewandte Festkörperphysik, Tullastrasse 72, D-79108 Freiburg, Germany. He is now with SDL, Inc, 80 Rose Orchard Way, San Jose, CA 95134-1365 USA.

Publisher Item Identifier S 1041-1135(96)07436-8.

The lasers used in this study were grown by molecular-beam-epitaxy on undoped GaAs substrates. A detailed description of the layer sequence, and of the DC and HF properties of the devices can be found elsewhere [6], [7]. In brief, the epilayer structure of these devices consists of four 5.7 nm $In_{0.35}Ga_{0.65}As$ QW's separated by 20 nm GaAs barriers, upper and lower 48-nm-thick GaAs confinement regions, and $Al_{0.8}Ga_{0.2}As$ cladding layers. Structures with three different doping levels were characterized: nonintentionally doped active region (sample "undoped"); 5×10^{18} cm^{-3} (sample "low-doped") or 2×10^{19} cm^{-3} (sample "high-doped") 4.5 nm wide Be-doped regions placed above each QW. Lasers were fabricated with 3- to 40-μm-wide mesas, and cleaved to a length of 200 μm. On-wafer measurements of both the magnitude and phase of the impedance were performed using a fully calibrated HP 8722A network analyzer up to frequencies of 40 GHz.

The HFEI measurements were analyzed by comparing them with the theoretical expressions we have previously reported [4]. We solved the three rate equations for a QW laser with carrier transport/capture effects and defined the electrical diode time constant τ_o as

$$\tau_o = \tau_{\rm cap} + \xi\tau_{\rm sc} \tag{1}$$

with $\tau_{\rm sc} = R_d \times C_{\rm sc}$, R_d the diode dynamical resistance and $\xi = \tau_{\rm esc}/(\tau_{\rm esc} + \tau_{\rm eff})$ below threshold and $\xi = 1$ above threshold. Neglecting the carrier recombination in the core, and introducing the approximation $\tau_{\rm esc} \gg \tau_o$, we obtained the following expressions for the laser impedance:

$$Z(\omega) = R_d \frac{1}{(1+j\omega\tau_o)} \times \frac{1+j\omega\tau_1}{1+j\omega\tau_{\rm eff}} \quad \text{with} \quad 1/\tau_1 = 1/\tau_{\rm eff} + 1/\tau_{\rm esc} \tag{2}$$

below threshold and

$$Z(\omega) = R_d \frac{1}{(1+j\omega\tau_o)} \times \frac{\omega_r^2 - \omega^2 + j\omega\gamma_1}{\omega_r^2 - \omega^2 + j\omega\gamma} \quad \text{with} \quad \gamma_1 = \gamma + 1/\tau_{\rm esc}. \tag{3}$$

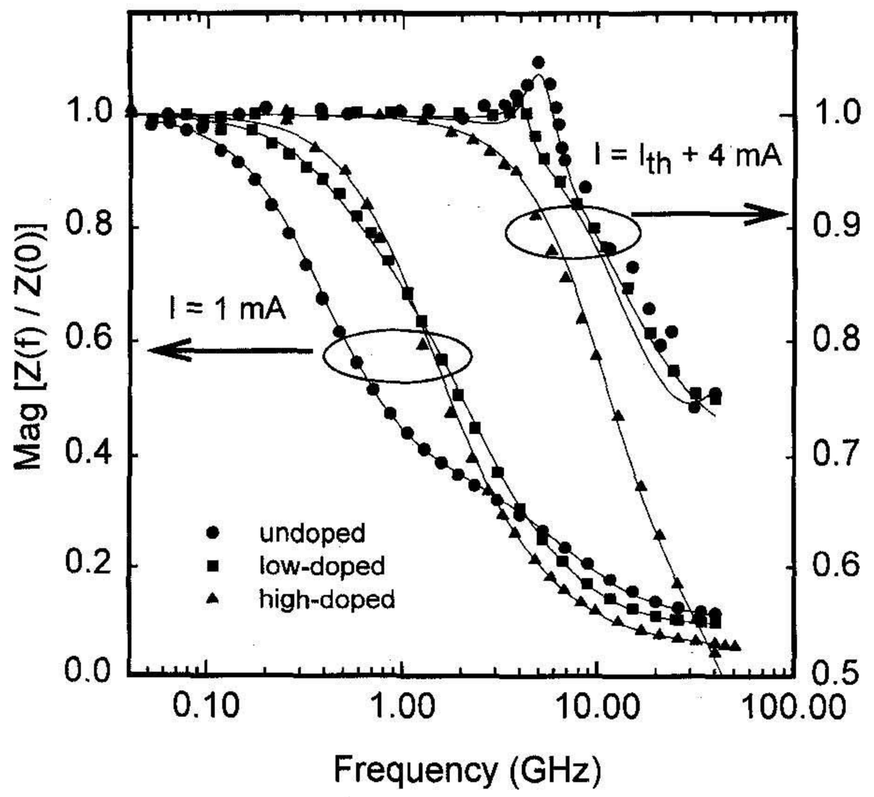

Fig. 1. Normalized magnitude of the impedance $\mathrm{Mag}\,[Z(f)/Z(0)]$ as a function of the frequency, at $I = 1$ mA and at $I = I_{\mathrm{th}} + 4$ mA, for 3 $\times$ 200 μm^2 lasers with the three different doping levels in the active region. Points are experimental data and lines are the best fit using the theoretical expressions described in text.

above threshold. In these equations, ω_r and $\gamma = 1/\tau_{\mathrm{eff}} + K/(4\pi^2) \times \omega_r^2$ denote the classical expressions for the relaxation oscillation frequency and damping rate in laser diodes, respectively, and K is the damping factor.

Fig. 1 shows the normalized magnitude of the impedance, $\mathrm{Mag}\,[Z(f)/Z(0)]$, below and above threshold, for lasers with different doping levels. A distinct behavior can be clearly observed: 1) below threshold, the impedance of the undoped sample shows an initial drop, almost a plateau, and a second drop (two real poles and real zero); the impedance of the high-doped laser has a 20 dB/dec roll-off (a real pole); and the impedance of the low-doped device shows an intermediate behavior; 2) above threshold, the impedances of the undoped and low-doped samples show a resonance peak, at a frequency corresponding to the relaxation oscillations, while the high-doped laser has again a real pole in the frequency dependent impedance.

These results can be interpreted with the help of (1)–(3) and considering the differences between the ratio $\tau_{\mathrm{esc}}/\tau_{\mathrm{eff}}$ for lasers with different doping levels.

1) *Undoped devices:* τ_{esc} is comparable to τ_{eff} (within an order of magnitude); (2) shows that $\tau_I \neq \tau_{\mathrm{eff}}$ and therefore the zero and the poles in the impedance below threshold lie at different frequencies. Above threshold expression (3) shows that $\gamma_I > \gamma$, and consequently the impedance has a peak at ω_r.
2) *High-doped devices:* τ_{eff} is much lower than τ_{esc}, therefore below threshold the zero at τ_I^{-1} and the pole at τ_{eff}^{-1} lie at the same frequency and cancel out; above threshold $\gamma_I \approx \gamma$, cancelling out the resonance terms in the numerator and denominator of (3). This yields an impedance with a single real pole at τ_o^{-1} both below and above threshold.
3) *Low-doped devices:* τ_{eff} is lower, but not much lower, than τ_{esc}. This implies that below threshold the impedance is an intermediate case between the two cases previously described; above threshold the resonance peak can still be appreciated, but with a lower height than in the case of the undoped device.

The exact small-signal solution of the rate equations for the magnitude and phase of the laser impedance, including a series resistance term, was fitted to the experimental results. As can be observed from the lines in Fig. 1, the fitting quality at frequencies lower than 20 GHz was very good. At higher frequencies a model with lumped circuit elements is no longer valid [8]. The extracted values for τ_{eff} were in good agreement with those obtained from measurements of the frequency dependence of the spontaneous emission [9], indicating the validity of pure electrical measurements for determining the carrier lifetime of QW lasers. A similar approach for bulk laser diodes has been recently proposed [10].

Fig. 2 shows the extracted values of τ_{esc} for undoped lasers as a function of the QW carrier density, which was calculated by integrating the carrier lifetime up to the bias current, and assuming a 100% injection efficiency. Within experimental error, the values of τ_{esc} for lasers with different cavity widths lie on a single curve, indicating the validity of the extraction method. τ_{esc} increases with the carrier density up to a saturation value of $\approx$0.7 ns. The observed dependence of τ_{esc} on the carrier density is attributed to the residual band bending of the p-n junction at the lower current levels through a higher tunnel-assisted re-emission rate. The values of τ_{esc} for the doped samples can not be directly determined from the fit of the theoretical impedance to the experimental results, but the absence of a clear zero in the impedance curves (see Fig. 1) indicates that $\tau_{\mathrm{esc}} \gg \tau_{\mathrm{eff}}$. Considering the values of τ_{eff} obtained for the doped samples from the modulation response of the spontaneous emission (typically 0.2 ns [9]), this yields a lower limit for τ_{esc} of 2 ns. The physical reason producing this increase of τ_{esc} with the p-doping concentration is not yet well understood, but it can be related to the deeper position of the electron quasifermi level at threshold in the doped lasers than in the undoped devices. The extracted values for τ_{esc} are more than one order of magnitude higher than those theoretically calculated considering carrier-polar longitudinal optical phonon interactions [11].

Fig. 3 shows the extracted values of τ_o as a function of the current for 3-μm-wide lasers with the three doping concentrations. The dependence of τ_o on the current, cavity width, and doping level can be well understood considering (1): τ_o arises from two different physical components: the effective capture time τ_{cap} and the time constant associated to the space charge capacitance τ_{sc}. The main dependence of τ_o on the current is due to the diode dynamical resistance R_d, which is proportional to I^{-1}, vanishing τ_{sc} at high current levels. Extrapolating the measured values of τ_o to infinite current we can roughly estimate the value of τ_{cap}, yielding $\tau_{\mathrm{cap}} \approx$ 2–5 ps. Our definition for τ_{cap}, given by the rate equations in [4], corresponds to the effective capture time defined in [3], i.e., $\tau_{\mathrm{cap}} = \tau_{\mathrm{dif}} + \tau_{\mathrm{capo}} \times (V_{\mathrm{core}}/V_{\mathrm{QW}})$, with τ_{dif} the carrier diffusion time, τ_{capo} the intrinsic quantum capture time, V_{core} the core volume and V_{QW} the QW volume. Assuming that the main component in τ_{cap} is the capture

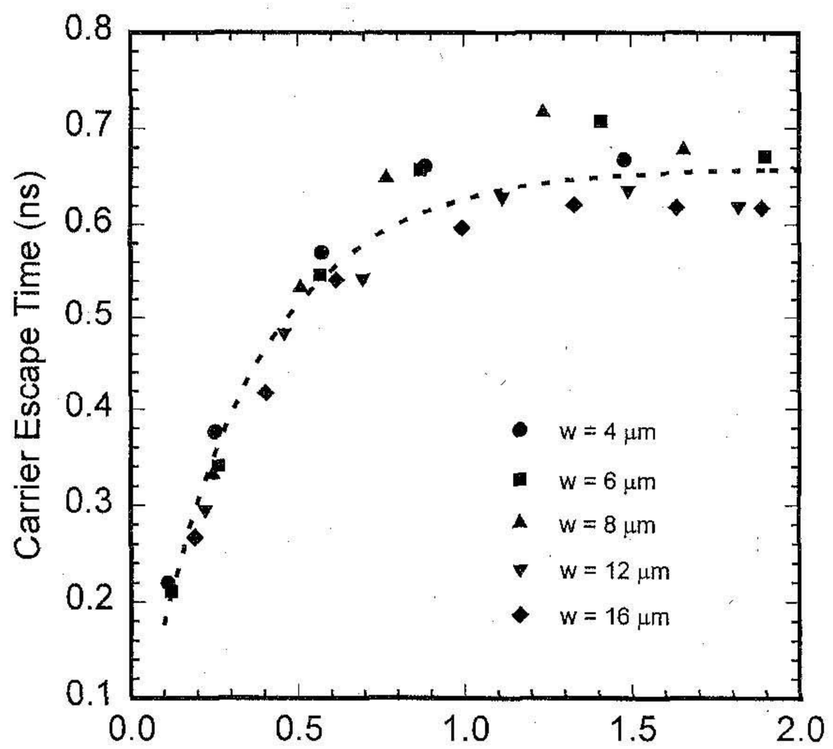

Fig. 2. Carrier escape time τ_{esc} as a function of the carrier density for undoped lasers with different cavity widths. Line is drawn as a visual aid.

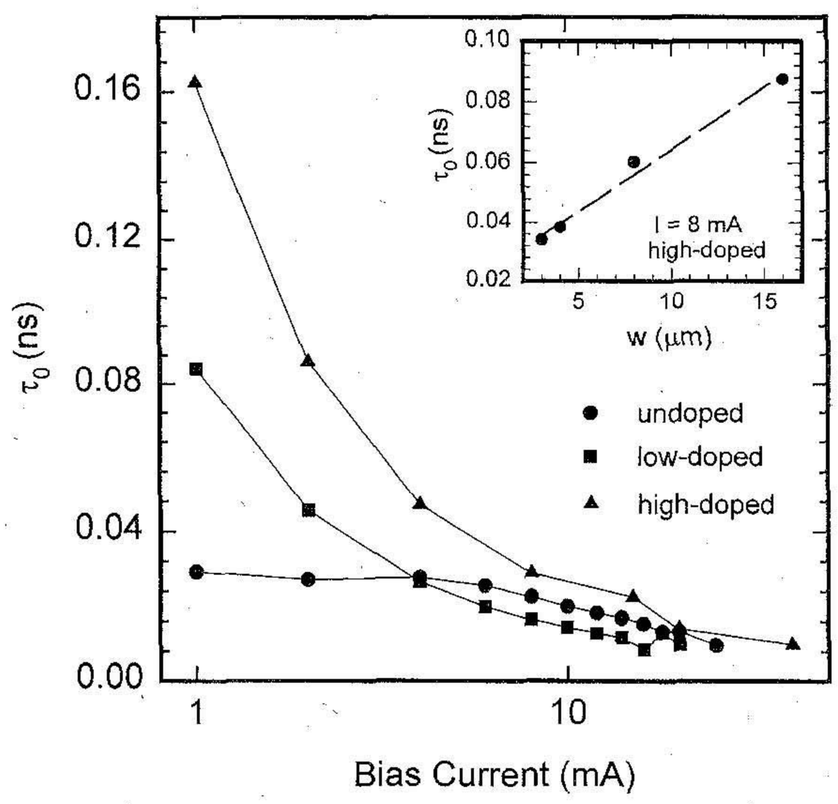

Fig. 3. Electrical diode time-constant τ_o as a function of the drive current for 3-μm-wide lasers with varied doping levels in the active region. Lines are drawn as a visual aid. The inset shows τ_o ($I = 8$ mA) as a function of the cavity width for lasers with high doping level in the active region; the line is the best linear fit to the data.

process, this yields $\tau_{capo} \approx 0.2$–0.5 ps. The increase in τ_o with the doping concentration is due to the increased values of C_{sc} at constant voltage [12] and of ξ in (1) for samples with high doping concentration. Expression (1) can be checked by comparing the measured values of τ_o for samples with different widths at low bias current ($\tau_{sc} \gg \tau_{cap}$, and hence $\tau_o \approx \tau_{sc}$), and considering that C_{sc} is proportional to the junction area. This has been done in the inset of Fig. 3, where we have plotted the measured values of τ_o at 8 mA for the high-doped lasers as a function of the cavity width, obtaining the predicted linear dependence. This result indicates that a new limitation should be taken into account when designing p-doped ultra-high-speed QW lasers: the addition of p-doping to the active zone increases the differential gain and decreases the damping factor K [6], but it also increases the value of τ_o, which introduces an additional roll-off into the modulation response [5].

In summary, we have performed and analyzed high-frequency electrical impedance measurements on high-speed MQW lasers with varied p-doping levels in the active region. We have shown that this measurement technique can provide valuable information about the time constants associated to the carrier dynamics. Our results demonstrate that in our laser structures the ratio τ_{cap}/τ_{esc} is much lower than the unity ($\sim$0.001–0.005), and that the addition of p-doping to the active region produces a substantial increase of the carrier escape time τ_{esc} (from 0.7 ns for the undoped devices to a value higher than 2 ns for the high-doped lasers).

Acknowledgment

The authors wish to thank W. Benz, J. Fleissner, E.C. Larkins, P. J. Tasker, B. Matthes, K. Räuber, K. Czotscher, and A. Schönfelder for their assistance with sample preparation and characterization. They also wish to thank G. Grau and H. Rupprecht for their continuing support.

References

[1] R. Nagarajan, T. Fukushima, M. Ishikawa, J. E. Bowers, R. S. Geels, and L. A. Coldren, "Transport limits in high-speed quantum-well lasers: experiment and theory," *IEEE Photon. Technol. Lett.*, vol. 4, pp. 121–123, 1992.

[2] W. Rideout, W. F. Sharfin, E. S. Koteles, M. O. Vassell, and B. Elman, "Well-barrier hole burning in quantum well lasers," *IEEE Photon. Technol. Lett.*, vol. 3, pp. 784–786, 1991.

[3] S. C. Kan, D. Vassilovski, T. C. Wu, and K.Y. Lau, "Quantum capture limited modulation bandwidth of quantum well, wire, and dot lasers," *Appl. Phys. Lett.*, vol. 62, pp. 2307–2309, 1993.

[4] S. Weisser, I. Esquivias, P.J. Tasker, J. D. Ralston, B. Romero, and J. Rosenzweig, "Impedance characteristics of quantum-well lasers," *IEEE Photon. Technol. Lett.*, vol. 6, pp. 1421–1423, 1994.

[5] S. Weisser, I. Esquivias, P. J. Tasker, J. D. Ralston, and J. Rosenzweig, "Impedance, modulation response, and equivalent circuit of ultra-high-speed $In_{0.35}Ga_{0.65}As$/GaAs MQW lasers with p-doping," *IEEE Photon. Technol. Lett.*, vol. 6, pp. 782–784, 1994.

[6] J. D. Ralston, S. Weisser, I. Esquivias, E. C. Larkins, J. Rosenzweig, P. J. Tasker, and J. Fleissner, "Control of differential gain, nonlinear gain, and damping factor for high-speed applications of GaAs-based MQW lasers," *IEEE J. Quantum Electron.*, vol. 29, pp. 1648–1659, 1993.

[7] I. Esquivias, S. Weisser, A. Schönfelder, J. D. Ralston, P. J. Tasker, E. C. Larkins, J. Fleissner, W. Benz, and J. Rosenzweig, "DC and high-frequency properties of $In_{0.35}Ga_{0.65}As$/GaAs strained-layer MQW laser diodes with p-doping," *Inst. Phys. Conf. Ser.*, no. 136, 1994, pp. 265–270.

[8] S. Weisser, I. Esquivias, P.J . Tasker, J. D. Ralston, and J. Rosenzweig, "Impedance, modulation response, and equivalent circuit of ultra-high-speed InGaAs/GaAs MQW lasers," in *Proc. IEDM Technical Meet.*, Washington, DC, 1993, pp. 601–604.

[9] K. Czotscher, "Systematische Untersuchung der effektiven Trägerlebendsdauer in InGaAs/GaAs-Lasern," Diplomarbeit, Universität Karlsruhe, 1994.

[10] G. E. Shtengel, D. A. Ackerman, and P.A. Morton, "True carrier lifetime measurements of semiconductor lasers," *Electron. Lett.*, vol. 31, pp. 1747–1748, 1995.

[11] C. Y. Tsai, C. Y. Tsai, Y. H. Lo, R. M. Spencer, and L. F. Eastman, "Nonlinear gain coefficients in semiconductor lasers: effects of carrier diffusion, capture, and escape", *IEEE J. Select. Topics Quantum Electron.*, vol. 1, pp. 316–330, 1995.

[12] S. M. Sze, *Physics of Semiconductor Devices*, 2nd ed. New York: Wiley, 1981.